

Effect of Multiple Heat Transfer Sources on Vaporization Rate of Liquefied Natural Gas Water Spills

Oluwapelumi Ezekiel Ishola*, Emeka Ogbuigba*, Adanna Chukwurah**, Emeka Joachim Okafor*

*(Department of Petroleum and Gas Engineering, University of Port Harcourt, Choba, Port Harcourt, Nigeria
(Email: emeka.okafor@uniport.edu.ng)

*(Department of Petroleum and Gas Engineering, University of Port Harcourt, Choba, Port Harcourt, Nigeria
(Email: ishpelumi@gmail.com)

** (Emogas Limited, Mgbuoba, Port Harcourt, Nigeria)
(Email: adanna.chukwurah@emogas-ngr.com)

*(Department of Petroleum and Gas Engineering, University of Port Harcourt, Choba, Port Harcourt, Nigeria
(Email: emeka.ogbuigba@uniport.edu.ng)

Abstract:

An LNG pool vaporization rate model is used to analyze the effect of multiple heat sources on the vaporization process. The heat sources include convection, conduction from dyke, conduction from tank, radiation, and conduction from water. It is found that the multiple heat source effect increases the rate of vaporization. The integrated spreading and vaporization rates model are solved analytically and implemented in FORTRAN. The overall results indicate, among other factors, that the magnitude of the heat flux into the pool will affect the vaporization rate and, therefore, multiple heat sources to the pool should be considered when predicting LNG pool vaporization rates.

Keywords — Heat transfer, vaporization rate, multiple heat transfer sources, LNG spills

I. INTRODUCTION

Modelling vaporization of hazardous fluids such as liquefied natural gas (LNG) can find its applications in consequence assessment of hazardous liquid spills on solid and liquid substrates. Vaporization rate modelling, a type of source term modelling, has undergone much study in recent years. In the spill modelling problem, liquid spill occurs upon rupture of containment with the fluid forming a pool on the substrate. Heat is then transferred into the spreading pool, resulting in the vaporization of the pool. The resultant vapour evolving from the vaporizing pool can disperse above the pool, in the absence of an ignition source. If the vapour-air mixture encounters an ignition source, a flash fire can result which can burn back towards the pool to form a pool fire. There are concerns of thermal radiation hazards associated with these pool fires and if these incidents occur

within complex geometries, a vapour-cloud explosion can result, thereby endangering life and property. The vaporizing pool and its simultaneous spreading, if unconfined, result in the so-called source-term problem involving simultaneous vaporization and spreading, and leading to vapour cloud dispersion.

LNG vapour cloud dispersion process requires clear understanding of fundamental physics for better quantification and control of the process. Sometimes, it is difficult to attain accurate vaporization. However, a one-dimensional (1-D) vaporization model helps in understanding the complex phenomena (Conrado and Vesovic, 2000; Vesovic, 2006). Models of risk based LNG spills and vaporization has been proposed by a number of workers (Abdulahi et al, 2022; Lervag et al, 2022; Nubli et al, 2024; Zhang et al, 2024; Fan et al, 2024; Vesovic, 2006; Conrado and Vesovic, 2000). This work will incorporate a multiple heat source

model for vaporization rate that will consider heat transfer to the pool from multiple sources other than from conduction through the substrate water. This new model is expected to improve the tracking of spreading and vaporization rate of the LNG pool, accounting for the effect of multiple heat flux densities on the pool. There are many parameters that have influences on the vaporization process and thereby the amount of vapour cloud that can evolve. Surface temperature, vaporization flux, pool thickness, are among. The objective of this paper is to study the effect of accounting for multiple heat transfer sources on LNG pool vaporization rate.

II. METHODOLOGY

A. Mechanism of LNG Spills

A schematic representation of the physical processes occurring following LNG spills is shown in Fig. 1. When LNG is released onto the surface of the water, a pool of LNG forms and spreads, vaporizing quickly and producing vapour (Wodek, 2019). The resultant liquid, which is mostly made up of methane, has several dangerous characteristics because of its cryogenic state and inflammable nature. When LNG is released into water, it will boil

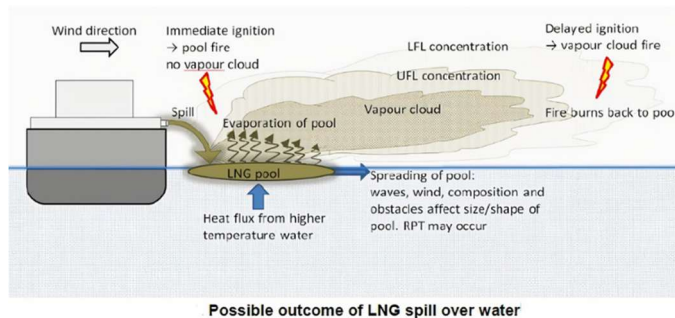


Fig. 1 : Physical processes of LNG spill over water

quickly and produce vapour, which will either disperse or condense into a dense white cloud. When there is a source of ignition, the LNG vapour may ignite if its concentration is within the flammability range, which can result in fires and explosions under specific situations (Vesovic, 2006; Conrado and Vesovic, 2000). Spilling LNG onto water forms a pool and the water surface acts as a heat source to cause the LNG pool to vaporize. Since LNG is less dense than

water, it will always create a buoyant pool on the surface of the water (Michelle et al., 2012).

B. Boiling Curve

In principle, LNG pool expands radially and boils in three successive regimes: the film boiling regime, the transition boiling regime, and the nucleate boiling regime (see Figure 2). LNG boiling is influenced by heat flux into the LNG pool from the underlying water. Figure 2 is a plot of heat flux, q , against temperature difference between LNG pool and water surface – the so-called boiling curve (Aursand, 2018). Observe the considerable dependence of the heat flux between a boiling liquid and a heat source on the temperature differential, ΔT .

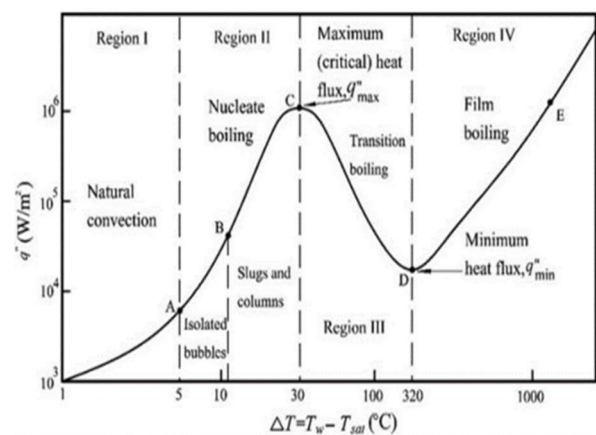


Figure 2: Boiling curve (Kulitsa and Wood, 2018).

In a case LNG boiling over water, a significant superheat, occurs at the start of the LNG pool formation on the water surface. A vapour film forms between the water's surface and the LNG pool, and the heat flux continuously decreases during the film boiling regime. Because the produced vapour layer keeps the LNG pool from coming into close contact with the water's surface, there is less heat transfer to the LNG pool, which reduces the amount of vapour generated (Vesovic, 2006; Conrado and Vesovic, 2000).

The gradual decrease in temperature is caused by the water surface heat loss and the cooling effect of cryogenic LNG. The start of the development of

vapour pockets is when the heat flux reaches a minimum (q_{min}) which occurs at or close to the, T_L ,

The minimum point temperature signals the start of the transition boiling regime, which is characterized by partial collapse and regeneration of the vapour layer as well as vapour pockets that provide partial contact between the LNG pool and the water's surface beneath (Vesovic, 2006; Ezeh and Okafor, 2022). The heat flux increases monotonically because of the enhanced contact between the LNG pool and the water's surface. This is anticipated to go on until the maximum or critical heat flux (q_{crit}), is reached. Beyond this point, the heat flux from the water surface to the LNG pool begins to decrease, signaling the start of the nucleate boiling regime characterized the vapour film has entirely collapsed, and there is the total collapse of the vapour film. A pure liquid substance's saturation or boiling point, such as methane, is dependent on the pressure that is applied (Bijoy et al., 2022).

It is important to develop methods for estimating the vaporization of LNG pools in order to conduct an acceptable risk assessment and consequence analysis of a potential LNG spill on water surface. An essential component of risk assessment and consequence analysis for a potential LNG leak on the water surface is modeling the vaporization rate of the LNG pool (Wodek, 2019 and Yi, 2012). In doing so, it is important to account for factors such as LNG pool height and multiple heat transfer sources on vaporization rate.

C. LNG Source Term Modelling: Spreading and Vaporization

Three basic processes are involved in an LNG spill over water: (1) pool spreading; (2) heat transfer; and (3) pool vaporization from the heating source to the LNG pool (Vesovic, 2006; Conrado and Vesovic, 2000).

(1) MODELLING POOL SPREADING

A spreading pool model exists to predict the spreading behaviour of the LNG pool (Velisa, 2006; Conrado and Vesovic, 2000). There are different regimes of spreading (Conrado and

Vesovic, 2000). The gravitational-inertial spreading regime is where surface tension and viscous forces will not become significant until the majority of the LNG has evaporated. (Otterman, 1975; Chang et al, 1982). If the ratio of the spreading fluid's density to the resisting fluid's is of the order of unity, the spreading rate will be determined by the leading front's velocity (Webber et al, 1986; Fannelop et al, 1972) or shallow layer theory (Webber et al, 1986), with the rate of spreading expressed as,

$$dR/dt = 1.64 \left[\frac{Mg(\rho_w - \rho)}{\pi\rho_w} \right]^{\frac{1}{2}} 1/R$$

where ρ and ρ_w are the densities of LNG and water, respectively, and Mg is the mass of liquid still in the pool.

(2) MODELLING HEAT TRANSFER

An LNG pool will absorb heat from multiple sources, all contributing to the vaporization of the pool and it is necessary to account for all these with good heat transfer model in order to improve the prediction of the rate of vaporization. In this work, the heat transfer from sources other than water is incorporated. Possible heat sources include: water, dike, storage tank, air and radiation. In the case of heat transfer from water to the pool, ice could form (Feldbauer, 1972; Otterman, 1975).

HEAT FROM WATER

The heat flux into the LNG, q , is provided by;

$$q = h(T_w - T) = h\Delta T \quad (2)$$

where ΔT is the superheat temperature in the context of this work, h is the heat transfer coefficient, and T and T_w are the cryogen and water temperatures, respectively. We assume boiling to occur only in the film boiling regime. (Collier & Thome, 1994). However, equation (2) is dependent on the thermophysical

characteristics of the fluids involved and, on boiling regime that takes place. The heat transfer coefficient (h_f) for film boiling in Klimenko's 1980 study is provided by (Conrado and Vesovic, 2000):

$$h_f = \lambda v Nu / l_c \quad (3)$$

LNG vapor's thermal conductivity, or λv , is 1.24×10^{-4} W/m.K. The critical wavelength of Taylor instability, denoted by l_c in the equation (4) below, is known as the Nusselt number, or Nu.

$$l_c = 2\pi[\sigma/g(\rho L - \rho v)]^{\frac{1}{2}} \quad (4)$$

LNG has a density of 423 kg/m³, ρL = surface tension of the liquid-vapour interface (0.014 N/m), and ρv = density of the LNG vapour film (0.657 kg/m³). Equation below provides the Nusselt number, Nu in equation (3) above for laminar vapour flow across layers of vapour film.

$$Nu = 0.19[ArPr]^{\frac{1}{3}} f_1 \quad (5)$$

In equations (6), (7), (8) and (9), Pr , is the Prandtl number of the vapour phase, f_1 , is the near-unity correction factor whose values depend on the superheat temperature and Ar , is Archimedes number

$$f_1 = 1 \text{ at } r/Cpv\Delta T \leq 1.4 \quad (6)$$

$$f_1 = 0.89(r/Cpv\Delta T) \text{ at } r/Cpv\Delta T > 1.4 \quad (7)$$

$$Ar = (2\pi)3\sigma^3/2/\rho v V v^2 \sqrt{g(\rho L - \rho v)} \quad (8)$$

When Ar is less than 10^8 , the Archimedes number, as stated by the previous expression (8), is such that vapour flow via layers of vapour film is laminar (Vesovic, 2006; Conrado and Vesovic, 2000). The vapour

phase viscosity, or Vv , is equal to 6.287×10^{-3} Ns/m². Prandtl Number, or Pr , is provided by

$$Pr = \mu v C_{pv} / \lambda v \quad (9)$$

μv is the viscosity of the vapour phase, $\mu v = 6.287 \times 10^{-3}$ Ns/m²; C_{pv} is specific heat capacity of LNG vapour, $C_{pv} = 2.087$ KJ/kgK at 200 K. The amount of heat transferred to the water's surface by LNG determines the temperature of the water's surface. The Fourier heat equation can be used to represent heat conduction through a body of water. It is assumed that the predominant mode of heat transfer direction is vertical upward, making the temperature distribution of the water one-dimensional (1-D), assuming that the water thermal boundary layer is small (Vesovic, 2006).

$$dT_w/dt = Kw(d^2 T_w/dy^2) \quad (10)$$

The thermal diffusivity of water is denoted by Kw , and its numerical value is 1.4558×10^{-7} m²/s. Next, the water surface temperature variation over time is provided by Vesovic (2006):

$$T_w = T_b + (T_o - T_b) \exp(-t^*) \operatorname{erfc}(\sqrt{t^*}) \quad (11)$$

where the reduced time, t^* , is given by

$$t^* = (h^2 / \lambda_w^2) Kw t \quad (12)$$

where T_o represents the water's initial temperature; T_w is the water's temperature at time t , T_b is the temperature at which LNG boils; and λ_w , or the water's thermal conductivity, is equal to 0.598 W/m K. There are several ways that energy can enter or exit a pool: convection, radiation, evaporation, and conduction. Furthermore, energy may be gained or lost by the pool in the form of perceptible heat. However, the end consequence will be the pool being in balance as stated by

$$q_{air} + q_{dike} - q_{evap} + q_{water} + q_{rad} + q_{tank} = 0 \quad (13)$$

HEAT FROM CONVECTION

It is easy to express the rate of convective heat transfer from the air to the pool as,

$$q_{air} = hA(T_{air} - T_{pool}) \quad (14)$$

where A is the surface area of the pool, T_{air} , is the Temperature of the air, T_{pool} is the temperature of the pool and h is the heat transfer coefficient of air (Cavanaugh, 1994).

HEAT FROM DIKE WALLS

The rate of heat transferred by contact with the walls of a containment dike is (Cavanaugh, 1994),

$$q_{dike} = \sum_{i=0}^N \frac{[2k(T_{dike} - T_{pool}) A_i]}{\sqrt{\pi\alpha(\sqrt{t} - \sqrt{t_i^*})}} \quad (15)$$

Throughout the simulation, the model maintains a steady, uniform dike temperature. From the expression " $\sqrt{t} - \sqrt{t_i^*}$ " t_i^* stays constant, the current time, t , will increase with time, with corresponding decrease in the rate of heat transfer.

HEAT FROM STORAGE TANK

The same formula that is used for q_{dike} can be used to express the rate of heat transmission by conduction through the storage tank (Cavanaugh, 1994).

$$q_{tank} = \sum_{i=0}^N \frac{[2k(T_{tank} - T_{pool}) A_i]}{\sqrt{\pi\alpha(\sqrt{t} - \sqrt{t_i^*})}} \quad (16)$$

HEAT FROM RADIATION

Another source of heat to the pool is the long wave radiation. The pool will either emit or absorb long wave radiation from the atmosphere based on the direction of heat flow. The radiation formula looks like this:

$$q_{rad} = \sigma \epsilon f_{area} (T_{air}^4 - T_{pool}^4) A. \quad (17)$$

where σ , is Stephen-boltzman constant, ϵ , is the emmissivity, and f_{area} , is the area factor.

The total heat transfer for the mutlti-source heat transfer model is given as;

$$q_{multi-source} = q_{water} + q_{convection} + q_{radiation} + q_{dike\ walls} + q_{storage\ tank} \quad (18)$$

(3) MODELLING POOL VAPORIZATION RATE

Equation 19 is an LNG pool vaporization rate model (Vesovic, 2006),

$$dM/dt = -m''R^2 \quad (19)$$

In equation (19), M is the mass of liquefied natural gas in kg; t is time in seconds; R is liquefied natural gas (LNG) pool radius, in m; while m'' is proportional to vaporization rate per unit area. Expressing equation 19 in terms of pool height gives,

$$-dH/dt = qx/\rho_{LNG}L_{LNG} \quad (20)$$

where H is the change in height of the LNG pool in meters; t is the time in seconds; qx is the heat flux in kJ/sec.m²; ρ_{LNG} is the density of LNG in kilograms per m³; and L_{LNG} is the latent heat of LNG vaporization in kJ/kg. A model is provided (equation 21) that takes into consideration the vaporization of LNG and the changes in pool height during an LNG spill on water surfaces.

$$dH/H = -qxdt/\rho_{LNG}L_{LNG} \quad (21)$$

(4) SOLUTION OF THE MODELS

The integrated model was solved and the FORTRAN tool in a stand-alone development environment used. Several simulations were conducted using an initial water surface temperature of 288 K to examine changes in the variables of interest. It was assumed that LNG is released at its boiling temperature of

112 K. At each time step, the changes in LNG height, water temperature, and vaporization flux/rate are calculated.

One way to simulate the vaporization of a liquid spill over time is to use successive time steps to calculate the system's state. Two requirements must be satisfied when determining the size of the time step: the simulation must be finished in a reasonable amount of time (which favors a big step size) and the computations must maintain accuracy (which tends to favor a small step size). Selecting a size that meets both goals is the tricky part. This simulation was done for 10,000secs to give an accurate reading.

III. RESULTS

Using the models described above, several simulations were run to determine how, given the same spill conditions, the rate of vaporization of LNG with heat transfer from water alone differs from that of LNG vaporization with heat transfer from other sources. The results for both cases are discussed in this section;

A. Case 1 – Single Heat Source Model

Figure 3 shows a rapid decrease in water surface temperature with time until the magnitude of the superheat decreases. Heat flux to LNG pool is shown in figure 4, suggesting that heat flux into the pool decreases with time since a decrease in the magnitude of the superheat is directly proportional to the heat flux density. Vapour production created a film that diminishes to a value of 1548.44kJ/m²s as shown in figure 4.

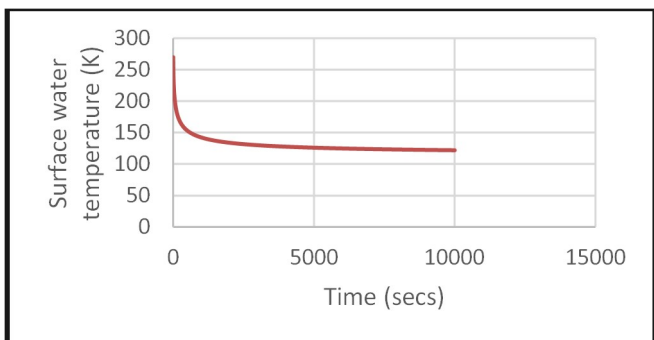


Figure 3. 1-D surface temperature profile

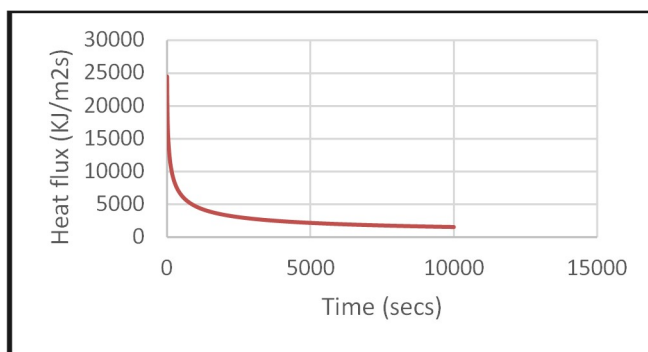


Figure 4. 1-D heat flux profile

Figures 5 and 6 below show the simulation results for the vaporization flux and LNG height, respectively. After 26 seconds, the vaporization flux reached its maximum values of 0.893 kg/m²s, while the LNG pool height peaked at 2.11 meters, and the vaporization flux achieved its maximum values at the same moment (26 seconds).

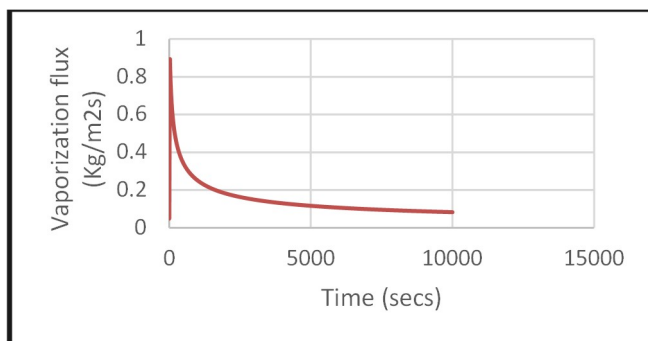


Figure 5. 1-D vaporization flux versus time profile

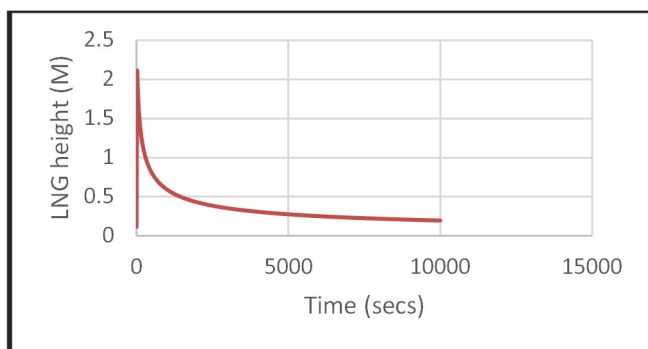


Figure 6. 1-D LNG height versus time profile

Timothy and Harri (2010) reported LNG vaporization rate's dependence on the height of the

LNG pool that is discharged into a limited water surface and this trend correlates with LNG vaporization flux/rate (Bijoy et al., 2022).

B. Case 2 – Multiple Heat Source Model

Figure 7 shows the heat flux profiles for case 1 and case 2, respectively. The maximum heat flux observed for case 1 is $244.84 \times 10^2 \text{KJ/m}^2\text{s}$ while the maximum heat flux for case 2 is $37334.01 \times 10^2 \text{KJ/m}^2\text{s}$. The heat flux for case 1 was observed to decrease slowly after the first 544 seconds following initial rapid reduction while for case 2, the heat flux began to slowly decrease after 162 seconds, thus suggesting a faster reduction in heat for case 2.

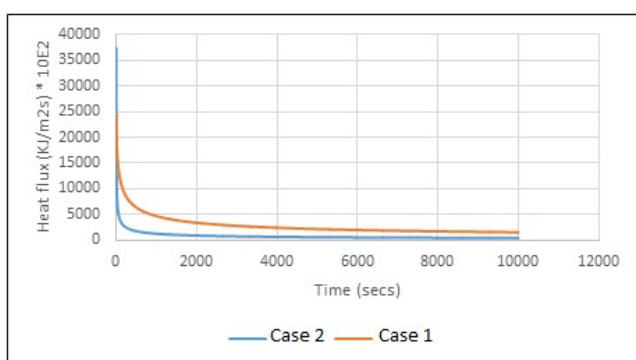


Figure 7: Heat flux profiles for case 1 and case 2.

Figures 8 and 9 represent the vaporization rate and LNG pool height behavior respectively for cases 1 and case 2.

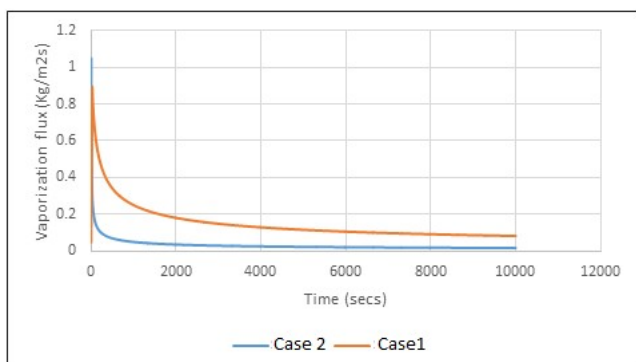


Figure 8. Vaporization flux versus time profiles for Case 1 and Case 2.

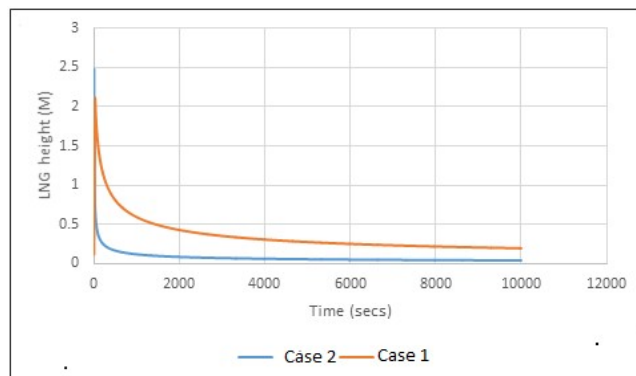


Figure 9: LNG pool height versus time profiles for Case 1 and Case 2.

IV. CONCLUSION

Effect of multiple heat sources on LNG pool vaporization rate is investigated. The cases where the LNG pool receives heat only from water and then from multiple sources are studied and compared. It is shown that the amount of heat and vaporization fluxes are relatively higher for case 2. Thus, the multi-heat source effect should be incorporated for an improved prediction of LNG pool vaporization rates.

REFERENCES

- [1] Aursand E. and Morten H., “Predicting triggering and consequence of delayed LNG RPT.” Article in *Journal of Loss Prevention in the Process Industries*, 2018.
- [2] Cavanaugh T. A., Siegell J. H. and Steinberg K. W., “Simulation of vapor emissions from the liquid spills,” *Journal of Hazardous Materials*, 38, 41-63, 1994.
- [3] Chang, H. R., & Reid, R. C., “Spreading-boiling model for instantaneous spills of liquefied petroleum gas (LPG) on water,” *Journal of Hazardous Materials*, 7, 19-35, 1982.
- [4] Cook J. and Woodward J.L., “A new integrated model for pool spreading, evaporation and solution on land and water,” *Health, safety and loss prevention in the oil, chemical and process industry*, (pp. 359-370) Oxford: Butterworth, 1993
- [5] Conrado C. and Vesovic V., “The influence of chemical composition on vaporisation of LNG and LPG on unconfined water surfaces,” 2000.
- [6] Ezeh E. A. and Emeka Okafor, “A Review of LNG Vaporization Rate Models for Water Spills,” *International Journal of Innovative Science, Engineering and Technology*, Vol. 09 Issue 11, 2022.
- [7] Klimenko V.V., “Film boiling on a horizontal plate - new correlation,” *Int. J. Heat Mass Transf.*, vol. 24, no. 1, pp. 69–79, Pergamon Press Ltd, Great Britain, 1980
- [8] Kulista M. and Wood D.A., “Floating storage and regasification units face specific LNG rollover challenges: Consideration of saturated vapor pressure provides insight and mitigation options,” *Natural Gas Industry B*, Volume 5, Issue 4, Pages 391-414, 2018.
- [9] Michelle M.F., Volkov D. and Analyst E., “LNG Safety and Security,” Centre for Energy Economics, Texas, USA, 2012
- [10] Shu Lj and Yonglin Ju, “Review of the LNG intermediate fluid vaporizer and its heat transfer characteristics,” 2021

- [11] Timothy L. M and Harri K.K., “The Effect of Turbulence on Rate of Evaporation of Cryogenic LNG and LN₂ on Water,” Texas A and M University, College Station, Texas, 2010.
- [12] Vesovic V. (2006), “The Influence of Ice Formation on Vaporization of LNG on Water Surfaces,” Department of Earth Science and Engineering, Imperial College London, London SW72BP, UK, 2006.
- [13] Abdullahi S. B. Gimba, Luqman B. Umdagas, Abdu Zubairu, Velisa Vesovic, Khadija S. Ibrahim, Ikechukwu Okafor, “Modelling LNG Spill on Water: Effects of Turbulence,” *Frontiers in Science* 2022, 12(1): 1-8 DOI: 10.5923/j.fs.20221201.01
- [14] Karl Yngve Lervåg, Hans Langva Skarsvåg, Eskil Aursand, Jabir Ali Ouassou, Morten Hammer, Gunhild Reigstad, Åsmund Ervik, Eirik Holm Fyhn, Magnus A. Gjennestad, Peder Aursand, Øivind Wilhelmsen, “A combined fluid-dynamic and thermodynamic model to predict the onset of rapid phase transitions in LNG spills,” *Journal of Loss Prevention in the Process Industries*, Volume 69, March 2021, 104354
- [15] Haris Nubli, Dongho Jung, Sang Jin Kim, Jung Min Sohn, “Structural impact under accidental LNG release on the LNG bunkering ship: Implementation of advanced cryogenic risk analysis,” *Process Safety and Environmental Protection*, Volume 186, Pages 329-347, 2024.
- [16] Zhaochen Zhang, Wei Zhu, Xuhai Pan, Bo Tan, Zhanjun Ye, Lifeng Zhang, Xianzu Zhou, Juncheng Jiang, “Field experimental study of high expansion foam coverage after LNG leakage,” *Process Safety and Environmental Protection*, Volume 183, Pages 315-326, 2024
- [17] Hongjun Fan, Xiangyang Xu, Nagi Abdussamie, Peggy Shu-Ling Chen, Andrew Harris, “Comparative study of LNG, liquid hydrogen, and liquid ammonia post-release evaporation and dispersion during bunkering”, *International Journal of Hydrogen Energy*, Volume 65, 2, Pages 526-539, 2024.